8th GRACM International Congress on Computational Mechanics
Volos, 12 July – 15 July 2015

# A MICRO-SCALE STRUCTURAL RESPONSE COMPARISON BETWEEN GFRP AND CFRP WIND TURBINE BLADES

**Efstathios E. Theotokoglou[1] and Georgios A. Balokas[2]**

[1]Department of Mechanics, Laboratory of Testing and Materials
School of Applied Mathematical and Physical Sciences, National Technical University of Athens
Athens, GR-15773, Greece
e-mail: stathis@central.ntua.gr ; web page: http://users.ntua.gr/stathis

[2]Department of Mechanics, Laboratory of Testing and Materials
School of Applied Mathematical and Physical Sciences, National Technical University of Athens
Athens, GR-15773, Greece
e-mail: g_balok@outlook.com

**Keywords:** Computational analysis, Composite materials, Fiber reinforced plastics, Failure criteria, Ply-drop analysis, Wind turbine blades.

**Abstract.** *Wind energy stands as one of the most important renewable energy sources. Large scale wind turbine blades are mainly based on fiber reinforced polymer composites, as an efficient way to further improve the performance of wind turbines is to reduce the weight of the blades. The problem of the interior support structure of a -high power- horizontal axis wind turbine blade is investigated in this study. A very detailed finite element model is developed, simulating the load-bearing box girder of the blade with a given airfoil shape, size and the type and position of the interior longitudinal beams and shear-webs. Previous work showed the challenging topics of material properties, design, computational analysis techniques and load response of a blade cross-section. In order to shed some light in a micro-scale level, a comparison of the most common composite blade materials (GFRP and CFRP) is presented, concerning stress and strain distributions but also displacements, which are critical for optimal blade design. A failure criterion is applied based on the shell finite element analysis of the model, in order to demonstrate the stress levels throughout the box girder and locate the initiation of fracture. Results concerning both glass and carbon materials are presented.*

## 1 INTRODUCTION

Wind energy is the fastest growing installed alternative-energy production technology, as it is credited with great advantages (i.e. no raw-material availability limitations, no toxic waste and no emission of carbon to the environment etc.). The strict environmental regulations along with the world's rapidly increasing energy needs and the depletion of fossil-fuels reserves, has brought the better handling of wind energy under assessment and consequently the continuous effort to improve wind turbine blades (WTB). Material selection of WTB is critical, as these structures should be stiff, strong and light in order to be efficient. Modern WTB are manufactured by hybrid materials which are consisted of polymer matrix composite materials, in a combination of monolithic (single skin) and sandwich composites. In this study a comparison is conducted between the behavior of glass and carbon fiber reinforced plastics (GFRP and CFRP), as the latter tend to dominate in very large blades.

Furthermore WTB include a lot of joints, where localized effects cause the initiation of stress concentrations that may influence the static and fatigue strengths of the composite and sandwich parts. The failure behaviour and the prediction of the proposed material systems using different failure theories are necessary for a complete investigation of WTB under combined loading. Thus, the subject of materials selection and computational analysis for a WTB is a currently developed research area [1-7], with the intention to investigate the behavior locally. In addition, some investigations deal with the very interesting subject of fatigue-life and failure prediction of the blade [1,2,3] combined with the numerical simulation [1,6,8] and the guidelines for design [1]. Remarkable results also come from studies concerning experimental full-scale tests [1,3].

The main objective of this study is to further advance the use of computer-aided engineering methods and tools (e.g. material-selection methodologies and geometrical modeling of the interior supporting structure) to the field of development of composite wind turbine blades based on advanced materials. Consequently, by using the quasi-static Finite Element Analysis (FEA) and a post-processing methodology, we investigate the behavior of the box girder of wind turbine blades under flap-wise loading for both GFRP and CFRP. From our computational analysis based on two dimensional (2D) and three dimensional (3D) Finite Element Models (FEMs), stress and displacement distributions are given and possible crack initiation positions are determined by implementing a composite materials failure criterion.

## 2 GEOMETRICAL MODEL AND MATERIALS

### 2.1 Geometrical Model

Turbine blades are perhaps the most critical components in the present designs of wind turbines. Among the main structural requirements for them are: (a) sufficient strength to withstand highly rare extreme static loading conditions, (b) sufficient blade flap-wise bending stiffness in order to maintain, at all times, the required minimal clearance between the blade tip and the turbine tower, (c) at least a 20-year fatigue life (under stochastic wind-loading conditions), and (d) various structural requirements related to a high mass of the WTB [3]. The WTB is essentially a cantilever beam mounted on a rotating hub (Fig. 1). The aerodynamic shape of the blade is formed by relatively thin outer shells. In order to reduce the self-weight bending moments in the blade section away from the blade root (the section where the blade is attached to the hub), blades are generally tapered. Tapering includes not only the blade cross section, but also the shell thickness (this ensures that different blade sections experience comparable maximum strains). In addition, blades generally possess a certain amount of twist along their length. Twist is beneficial with respect to self-starting of the rotor and through the bending/torsion coupling effects helps improving wind power capture efficiency [5].

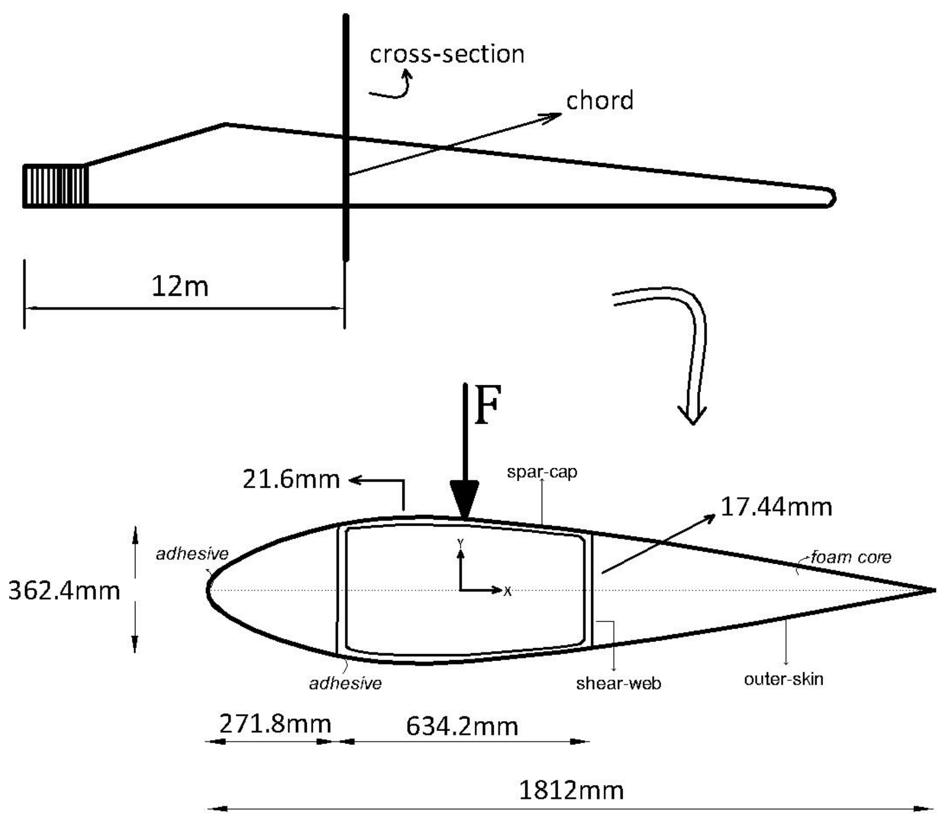


Figure 1: Blade geometry, position, dimensions and type of loading at the cross-section

Regarding the internal design of the blade, there are currently two major design tendencies: (a) the so-called one-piece construction and (b) the so-called two-piece construction [5]. The two designs differ with respect to the topology and joining of their load-bearing interior structure. In the case of the one-piece construction, the supporting structure consists of a single, close box spar (box girder) which is adhesively joined to the lower and upper outer shells. Since the stresses being transferred between the outer shells and the spar are low in magnitude, a lower-strength adhesive like polyurethane is typically used. A similar case is presented in Fig. 1, which is the one that concerns this study.

Focusing on the cross-section and the box-shape spar we observe two vertical shear webs, located at distances equal to 15% and 50% of the section-chord length (represented with a dotted line in Fig. 1), as measured from the leading edge. The webs are linked with two other stiffeners, the so-called spar-caps. A substantial build-up is located in the spar-cap thickness between the two vertical shear webs. More thorough examination of the blade construction, suggests that due to a relatively large spar-cap width and laminate thickness, good flap-wise bending strength is expected. This has been attained with the decrease of the flap-wise bending strength which could be increased provided that the shaft portion of the shear web had been placed at the section of the blade associated with the largest blade thickness.

### 2.2 Materials

For the development and manufacture of satisfactory products at minimum cost, it is important to make a sound, economic choice of materials. Any WTB material selection has the following requirements: (a) high material stiffness to maintain optimal shape of performance, (b) low density to reduce gravity forces and (c) long fatifue life to reduce material degradation. Modern composite materials such as GFRP and CFRP, have currently replaced traditional wooden or steel units. The fibers and the matrix materials like polyesters, vinyl esters, epoxies etc. are combined into these composites, offering good mechanical, thermal and chemical properties. Most glass-reinforced products are made with E-glass (electrical glass), which has good electrical and mechanical properties and high heat resistance. As for carbon fibers, they have become of increasing interest recently because of their decreasing price and their excellent combination of very high stiffness, high strength, light weight and low density.

This study in based on the current innovative manufacturing technologies [4,8]. The exterior airfoil skins and the interior vertical shear webs are constructed using a sandwich-like material consisting of (-45°/0°/45°) tri-axial fiber-glass composite laminate face-sheets separated by a balsa-wood core, to increase the buckling resistance. The spar caps are constructed of alternating equal thickness layers of the tri-axial laminates described above, and unidirectional laminates making the contribution of 0° laminate and the off-axis laminate 70% and 30%, respectively, to provide for bending stiffness and buckling resistance [4]. A summary of the composite laminate lay-up sequences and ply thicknesses used in different sections of the blade design is provided [5]. All the aforementioned composite laminates were based on epoxy matrix reinforced with E-glass and carbon fibers. As far as the adhesive layers (Fig. 1) connecting the spar-caps to the interior faces of the skin are concerned, they were taken to be epoxy based. A summary of the stiffness, mass and composite mixture properties (where applicable) of the applied materials, are provided in Table 1. In that table, $E_{xx}$ is the axial Young's modulus, $E_{yy}$ is the transverse Young's modulus, $G_{xy}$ is the in-plane shear modulus, $v_{xy}$ is the Poisson's ratio, $v_f$ is the fiber volume fraction, $w_f$ is the fiber weight fraction, and ρ is the density.

| Property | Uni | | Tri | | Random | | Balsa | Gel | Epoxy adhesive |
|---|---|---|---|---|---|---|---|---|---|
| | E-glass | Carbon | E-glass | Carbon | E-glass | Carbon | | | |
| $E_{xx}$ (GPa) | 31.00 | 146.00 | 24.20 | 65.00 | 9.65 | 62.47 | 2.07 | 3.44 | 2.76 |
| $E_{yy}$ (GPa) | 7.59 | 18.53 | 8.97 | 22.50 | 9.65 | 62.47 | 2.07 | 3.44 | 2.76 |
| $G_{xy}$ (GPa) | 3.52 | 9.41 | 4.97 | 13.46 | 3.86 | 24.19 | 0.14 | 1.38 | 1.10 |
| $v_{xy}$ | 0.31 | 0.27 | 0.39 | 0.29 | 0.30 | 0.29 | 0.22 | 0.30 | 0.30 |
| $v_f$ | 0.40 | 0.2 | 0.40 | 0.2 | - | - | - | - | - |
| $w_f$ | 0.61 | 0.6 | 0.61 | 0.6 | - | - | - | - | - |
| ρ (g/cm$^3$) | 1.70 | 1.75 | 1.70 | 1.75 | 1.67 | 1.73 | 0.14 | 1.23 | 1.15 |

Table 1: Material properties

## 3 COMPUTATIONAL PROCEDURES

### 3.1 Assumptions

The cross-section selected for modeling is based on experimental data [5], indicating that the part of the blade from the root of the supporting structure until the middle is the most critical for failure. As shown in Fig.1 the chord length of the cross-section (located at a distance of 12m from the root) is 1.812m, the thickness of the shear web is 17.44mm and the thickness of the spar-cap 21.6mm. The effective wind direction as comprehended by the WTB is in the rotational plane of the rotor, although the real-wind direction is orthogonal to it, since they are generally oriented in such a way that their wide faces are facing the wind. This type of loading causes the so-called flap-wise bending of the blades. This study only implements static, flap-wise loading, because it is generally the cause of failure for the blade and affects its behavior much more than the other types of loading (i.e. gravity loads, centrifugal loads etc.). The load magnitude is 16.25N/mm so that the results are comparable with other experimental and theoretical data, from previous analyses [1,6].

It has been experimentally demonstrated that the interior supporting structure (box-shape spar) is the first to reach failure. Thus, and because we are only interested in the transverse direction, it is considered proper to investigate the box girder alone. We assume that the box girder section is loaded with a line load in the center of the spar-cap, as shown in Fig. 1, which represents flap-wise type of loading. In order to simplify the complexity of the analysis, symmetry is assumed for the box girder cross section about both main axes (X, Y) (Fig. 1). Firstly, solid models with plane stress and plane strain assumptions were considered in order to investigate stress and displacement fields in detail. Furthermore, seeking to include 3D effects, we compare the results with shell models which are typically used for practical design. With the above simplifications, only a quarter of the entire cross-section of the box girder has been analyzed under the boundary conditions of Table 2, that refer to the global coordinate system of Fig. 1. The *u/v/w* symbol refers to translation in the X/Y/Z-direction and $\theta$ to rotation with respect to X/Y/Z-axis respectively.

| Area | u | v | w | $\theta_x$ | $\theta_y$ | $\theta_z$ |
|---|---|---|---|---|---|---|
| Cap (middle) | X | √ | x | x | x | x |
| Web (middle) | √ | x | x | x | x | x |

Table 2 : Model boundary conditions (x: restrained, √: unrestrained)

### 3.2 FEA Simulation Techniques

The finite element computer software ANSYS 14.5 [9] was used for the analysis. Regarding the solid, plane model, the so-called *plane 183* finite element was used, which is a two dimensional (2-D), 8 node quadrilateral (or 6 node triangular for irregular mesh), structural, solid element with the nodes located on its vertices and on the middle of its sides [9]. The primary objective was to describe the distribution of the stresses and the displacements in three different locations of the model: (A), (B) and (C) (Fig. 2). A very interesting problem arises for the modeling of the transition segment between the spar-cap and the shear-web. In our study ply-drop analysis (which is a common, practical design technique) was used to simulate the change of the laminate plies and the thickness reduction between the two areas. A very fine mesh is needed (Fig. 3) in order to realistically represent the sandwich and laminate joint of the structure.

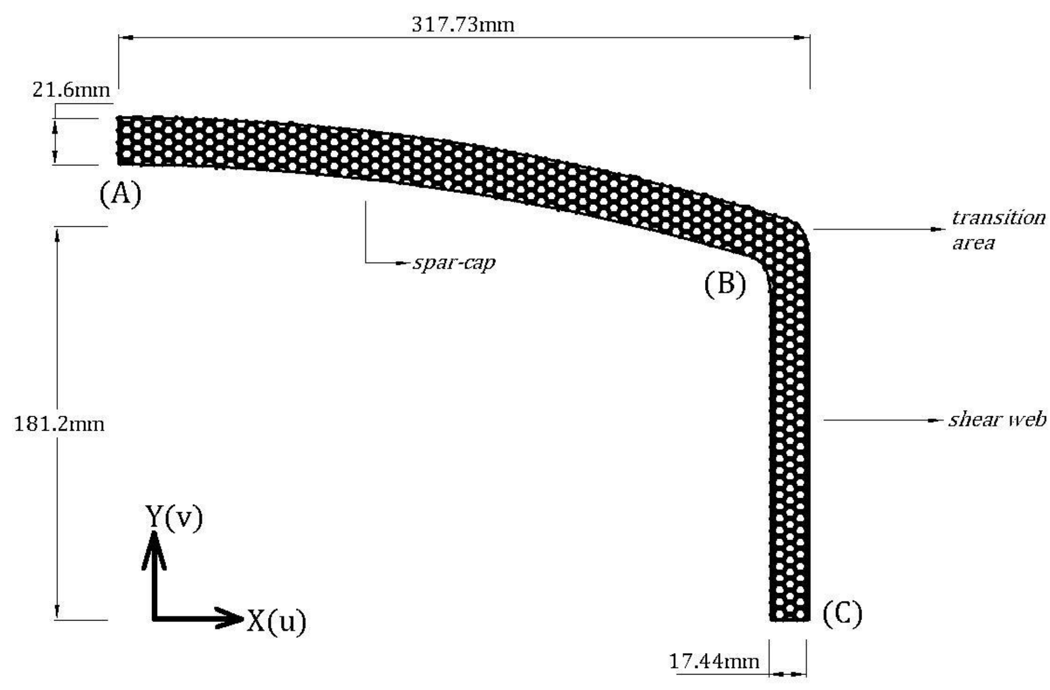


Figure 2: Solid, plane finite element model

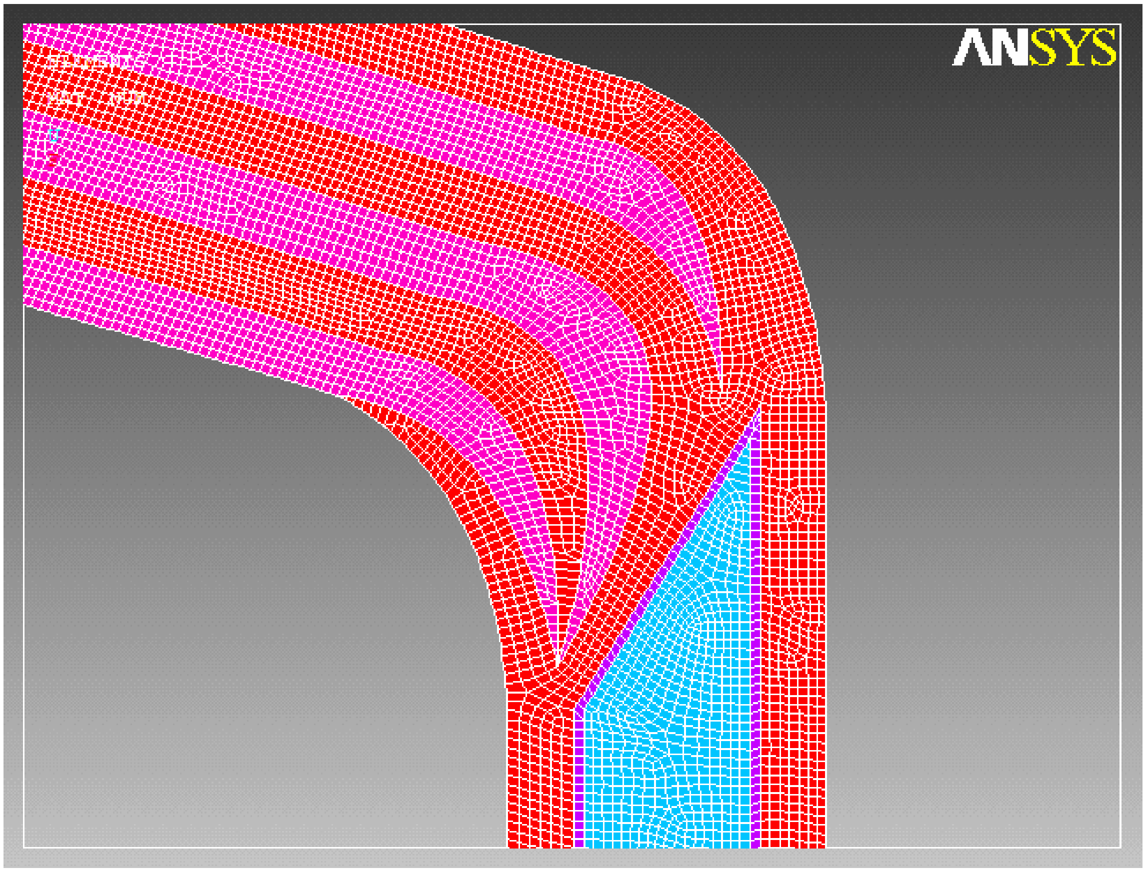


Figure 3: Solid plane finite element mesh with ply-drop at area B

Regarding the 3D simulation approach, the so-called *shell 281* finite element [9] was used, which is suitable for analyzing thin to moderately-thick shell structures. This particular element has eight nodes with six degrees of freedom at each node: translations in the x, y, and z axes, and rotations about the x, y, and z-axes. It may be used for layered applications for modeling composite shells or sandwich constructions. This is a typical FE modeling technique in practice because shell models are coarse, thus faster to compute. The 3D model is presented in Fig. 4.

A comparison between the 2D solid GFRP model and the shell GFRP model is presented in a previous study [5], at the three areas of the model for the calculated stresses (Fig. 2). At the symmetry planes the structure is only subjected to bending and the different models are found to give very similar predictions for the normal stresses $\sigma_{xx}$ and $\sigma_{yy}$, accordingly. The maximum normal stress appeared at the top of flange which is the point where compressive failure actually starts since there is a joint to the outer skin (Fig. 5). At area B, the structure is subjected to both bending and shear. The relatively simple shell models do not have the ability to predict well highly localized deformations and stresses, since they have been build to represent the global behaviour of structures. This should be taken into account when using strain and stress results from shell models in the practical design of structures. On the contrary, ply-drop analysis of plane elements offers satisfactory convergence and a quite smooth stress distribution, with no stress intensity spots (hot spots) for the design. Calculated displacements revealed no significant discrepancies between the two different computational techniques [5].

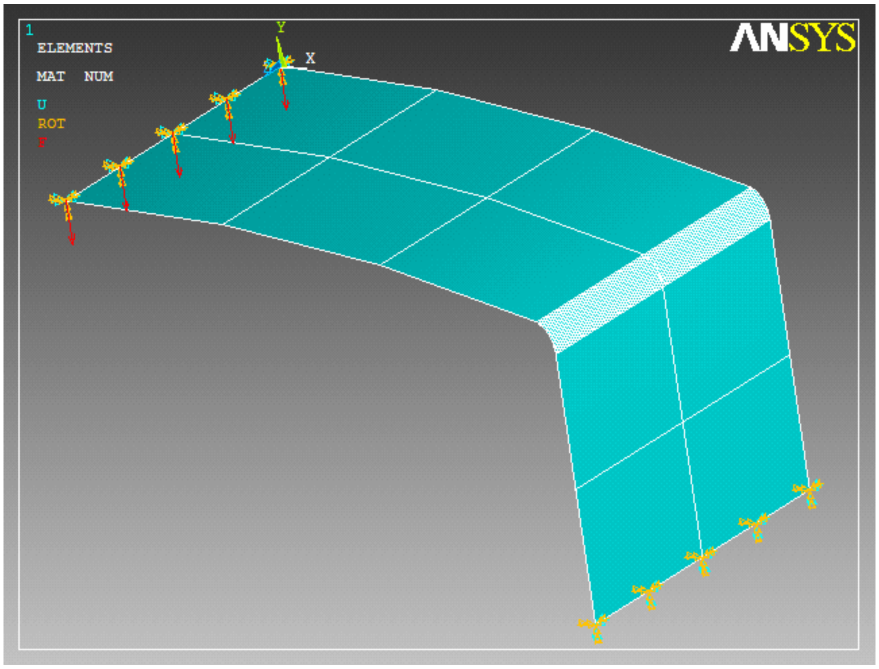


Figure 4 : Shell finite element model

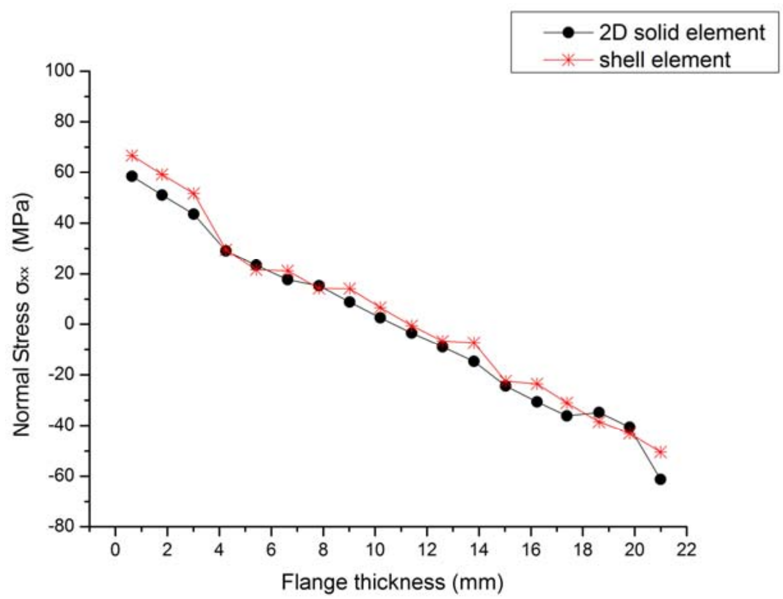


Figure 5: Stress $\sigma_{xx}$ at area A

### 3.3 Glass and Carbon Fibers Comparison

Over the years the size of WTB keeps growing, because of the need for maximum power. The size increase leads to self-load increase and as a result, to requirement for a more stiff blade (both flap-wise and edge-wise). The use of carbon fibers is inevitable in order to confront larger WTB, since they are much stiffer than glass fibers. A comparison is performed between GFRP and CFRP based on our shell finite element model. The same epoxy-based matrix was used with the replacement of carbon fibers characteristics instead of E-glass. Discrepancies between the stress distributions are insignificant (slightly greater stresses for the CFRP in specific thickness areas). Figures 6-8 present stress plots for all three analysis areas.

The expected result of the comparison -based on the carbon material properties presented in Table 1- was remarkable displacement reduction. The results for the displacements are very satisfactory as shown in Table 3, since the reduction in the blade displacements concerning areas A (spar-cap) and C (shear-web) present large discrepancies of the 74%.

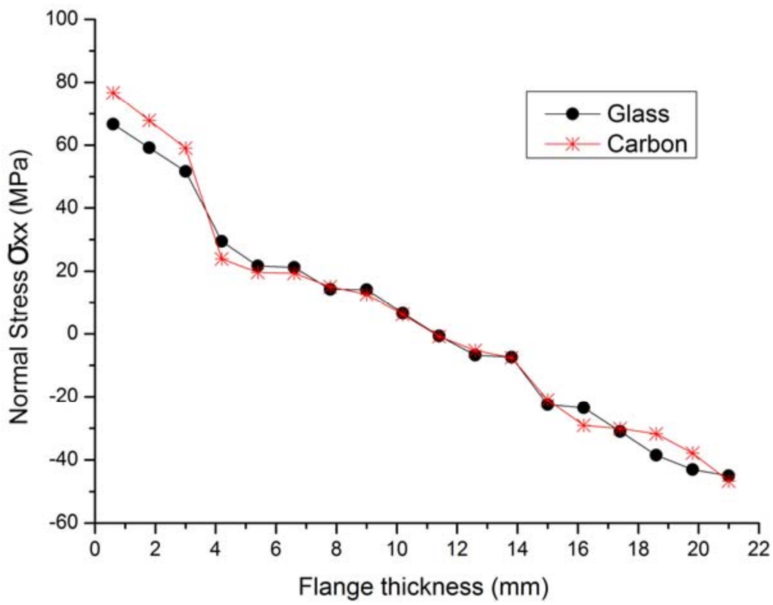


Figure 6: Stress $\sigma_{xx}$ at area A

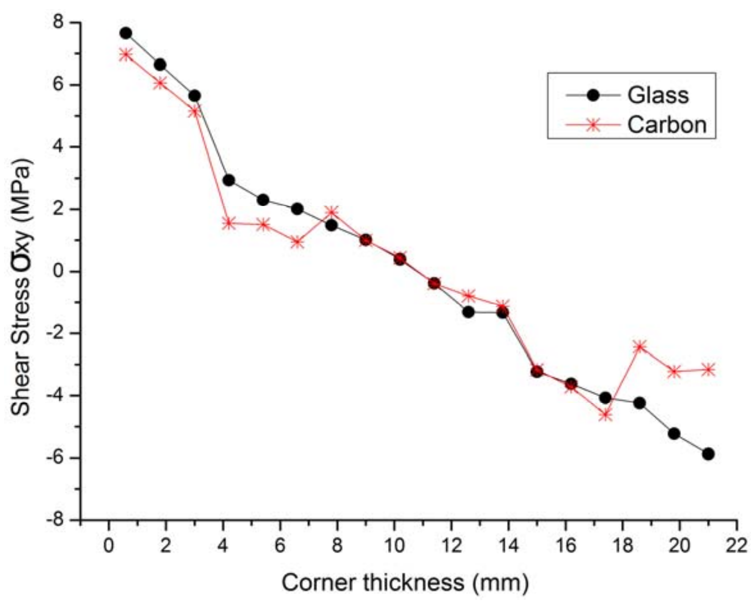


Figure 7: Stress $\sigma_{xy}$ at area B

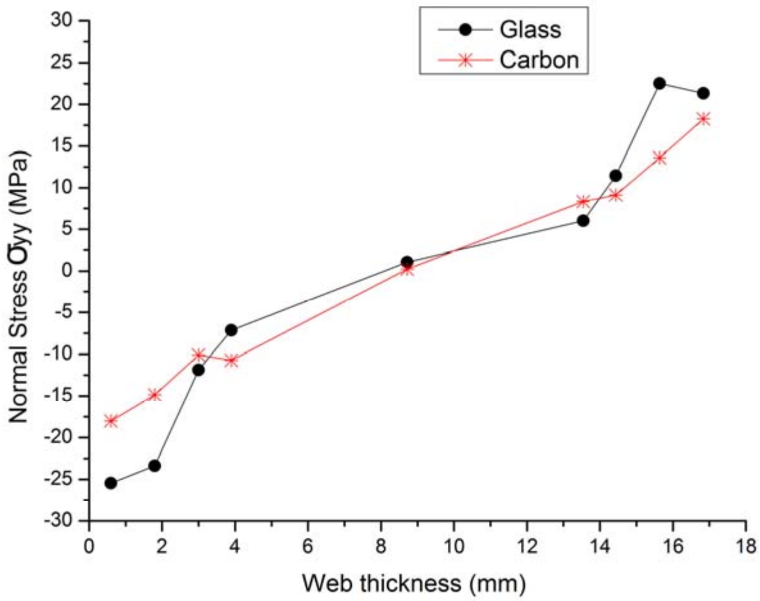


Figure 8 : Stress $\sigma_{yy}$ at area C

| | Glass/epoxy | Carbon/epoxy | reduction |
|---|---|---|---|
| Area A (mm) | -5.688 | -1.484 | -73.9% |
| Area C (mm) | 3.192 | 0.870 | -72.7% |

Table 3: Displacement comparison between GFRP and CFRP

### 3.4 Failure Criterion

With the given stresses in every ply of the model, it is useful to apply failure criteria for the orthotropic materials of the WTB in order to predict possible failure. Thus, we can reach to conclusions regarding the magnitude of the applied stresses, but also the plies of the composite materials (which ply is the weakest/strongest and which is the critical load for failure). In this study the Tsai-Wu [10] quadratic failure criterion is applied (a quite reliable criterion for 3D stress state) which is commonly used for orthotropic composites. The general expression is:

$$F_{ij}\sigma_i\sigma_j + F_i\sigma_i \leq 1 \ , \ \text{i,j=x,y} \tag{1}$$

The strength parameters $F_{ij}$ and $F_i$ included in the above equation are obtained from uniaxial and shear tests in terms of X, Y, X', Y' and S (X, Y: tension, X', Y': compression, S: shear) whose values are given in Table 4 [10]. Since Tsai-Wu criterion concerns only one of the plies of the composite laminate, it is used to check for possible ply failure, or alternatively which ply fails first for a certain load. Plies with fibers oriented vertically to the load direction are more likely to fail. A laminate material could not completely fail even though one or more of its plies have reached failure. Gradually, as more plies begin to fail the behaviour of the material changes, due to the stiffness reduction (although the material can still possibly bear loads, but with much larger deformation).

| | E-glass/epoxy (MPa) | Carbon/epoxy (MPa) |
|---|---|---|
| X | 1062 | 1830 |
| X' | 610 | 1096 |
| Y | 31 | 57 |
| Y' | 118 | 228 |
| S | 72 | 71 |

Table 4: Failure stresses for GFRP and CFRP materials

The critical load was investigated with inremental load increase until one of the plies reaches failure. For E-glass fiber model, ply failure was reached for a load of 49N/mm at areas A and C (spar-cap and shear-web respectively), as shown in Fig. 9. Specifically at the spar-cap area (laminate composite) the 15th ply failed (fibers oriented -45°) and at the shear-web area (sandwich composite) the exterior ply failed (fibers oriented 45°). Oppositely, for the CFRP model the highest ratio was observed at the exterior ply of the sandwich material of the shear web only. The critical load was 43.225N/mm (Fig. 10), slightly smaller than the CFRP critical load but without simultaneous failure of the spar-cap ply. The reason is the rather low shear strength of carbon in comparison to the rest critical stresses (Table 4), since there is strong interaction of shear and normal stress at the shear-web area.

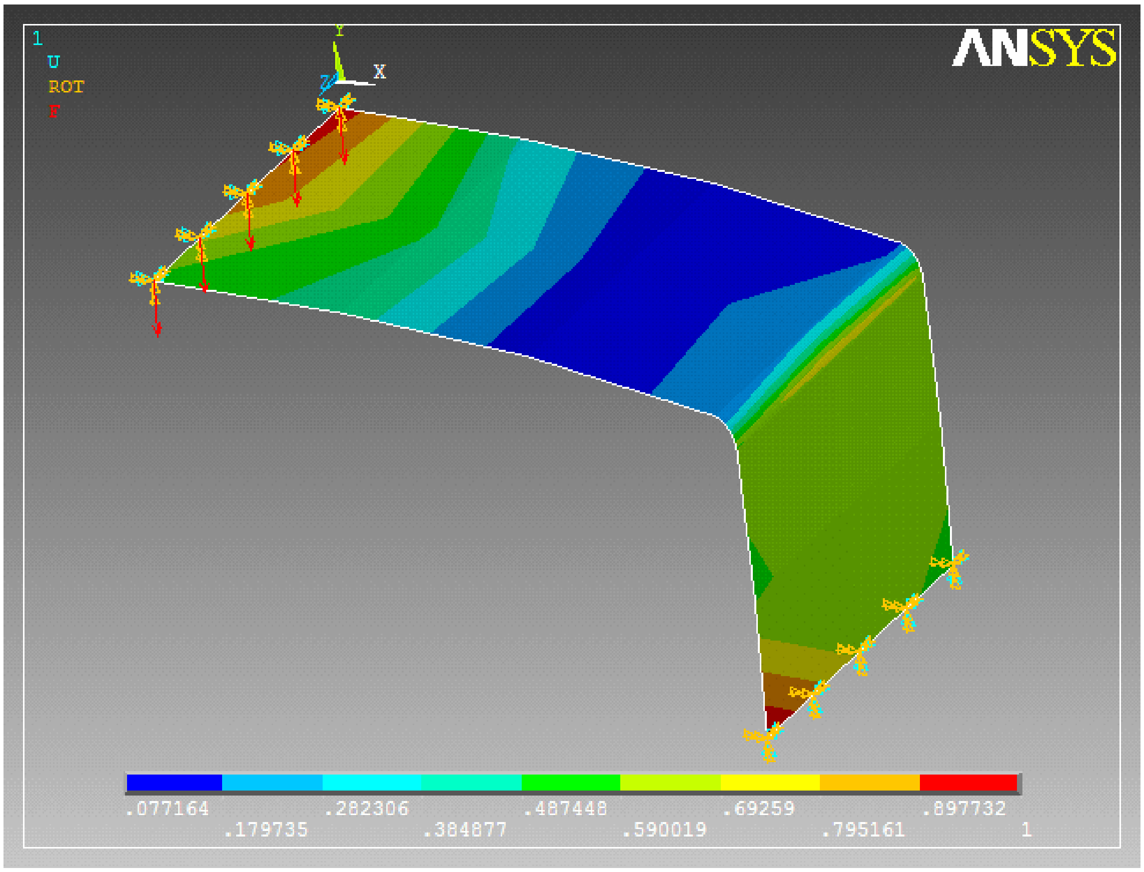


Figure 9 : Tsai-Wu criterion for GFRP (Load N=49N/mm)

## 4 CONCLUSIONS

This study investigates the behavior of a WTB cross-section at a micro-scale level, by directly comparing the most common innovative materials of current manufacturing technologies (GFRP and CFRP). The comparisons of materials as well as the implication of a failure criterion were performed using 3D shell elements, as they present good accuracy at the pure bending areas of the cross-section (which appear the higher stress levels). Stress distribution showed no significant deviation between glass and carbon fibers, in contrast to displacements. It should be highlighted that the stiff carbon fibers offered a deflection decrease of the order 74% at the box girder. Furthermore, due to their relatively low shear strength, carbon fiber plies provided a lower critical load in comparison to E-glass fibers. Nevertheless, this discrepancy may be of less significance in contrast with the box girder stiffness provided, regarding the benefits of the global behavior of the WTB structure.

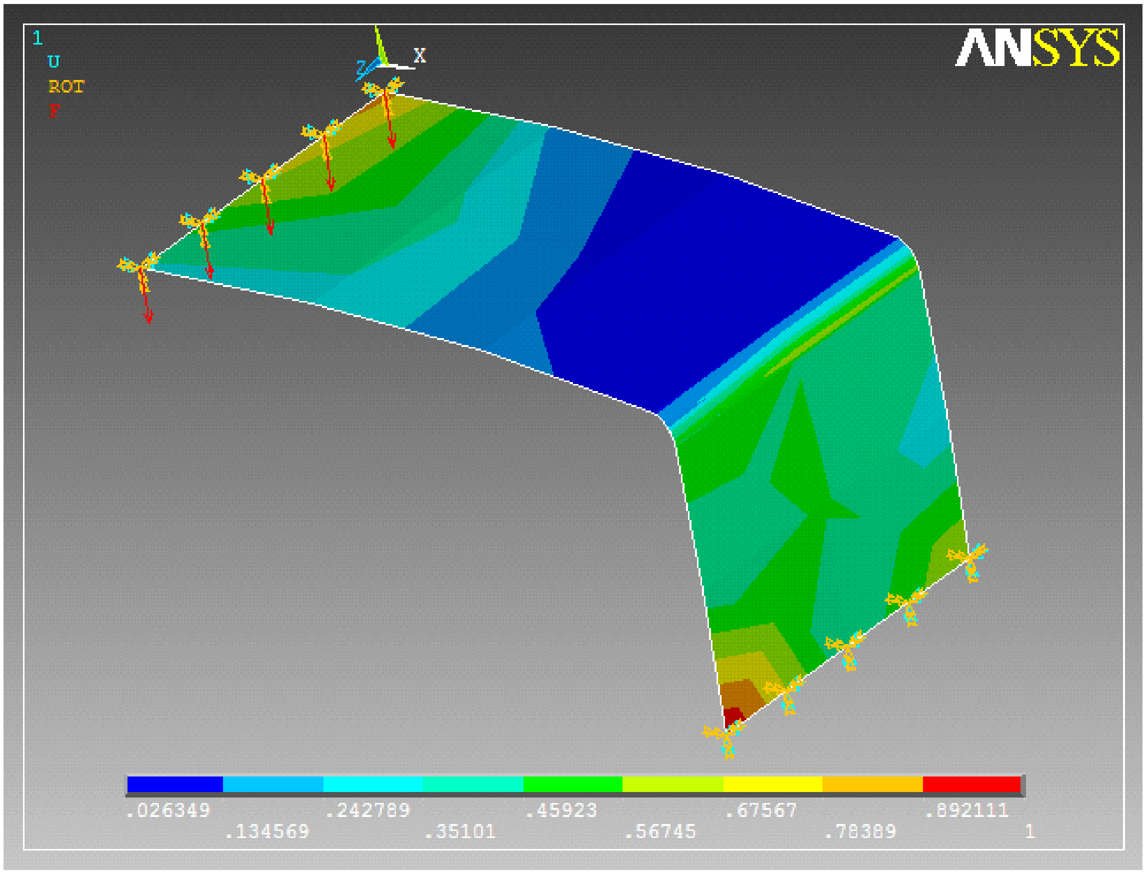


Figure 10: Tsai-Wu criterion for CFRP (Load N=43.225N/mm)

**REFERENCES**

[1] Jensen, F.M., Falzon, B.G., Ankersen, J., and Stang, H. (2006) "Structural Testing and Numerical Simulation of a 34m Composite Wind Turbine Blade", *Composite Structures*, Vol. 76, p.p. 52-61.

[2] Rajadurai, J.S. and Thanigaiyarasu, G. (2009), "Structural Analysis, Failure Prediction, and Cost Analysis of Alternative Material for Composite Wind Turbine Blades", *Mechanics of Advanced Material and Structures*, Vol. 16, p.p. 467-487.

[3] Grucijic, M., Arakere, G., Subramanian, E., Sellappan, V., Vallejo, A., and Ozen, M. (2009), "Structural-Response Analysis, Fatigue-Life Prediction, and Material Selection for 1 MW Horizontal-Axis Wind Turbine Blades", *Journal of Materials Engineering and Performance*, Vol. 19, p.p. 790-801.

[4] Thomsen, O.T. (2009), "Sandwich Materials for Wind Turbine Blades – Present and Future", *Journal of Sandwich Structures and Materials*, Vol. 11, p.p. 7-27.

[5] Theotokoglou, E.E., and Balokas, G.A. (2015), "Computational Analysis and Material Selection in Cross-Section of Composite Wind Turbine Blade", *Journal of Reinforced Plastics and Composites*, Vol. 34(2), pp. 101-115.

[6] Pardo, D.R. and Branner, K. (2005) "Finite Element Analysis of the cross-section of Wind Turbine Blades; a Comparison between Shell and 2d-Solid Model", *Wind Engineering*, Vol. 29, p.p. 25-32.

[7] Bozhevolnaya, E., Lyckegaard, A. and Thomsen, O.T. (2005) "Localized Effects Across Core Junctions in Sandwich Beams Subjected to in-Plane and Out-of-Plane Loading", *Applied Composite Materials*, Vol. 12, p.p. 135-147.

[8] Overgaard, L.C.T., and Lund, E. (2010) "Structural Collapse of a Wide Turbine Blade. Part B: Progressive Interlaminar Failure Models", *Composites Part A: Applied Sciences and Manufacturing*, Vol. 41, p.p. 271-283.

[9] ANSYS Engineering Analysis System, User's Manual, Swanson Analysis System Inc., (2010).

[10] Kollar, L.P. and Springer, G.S. (2003) "Mechanics of Composite Structures", *Cambridge University Press*.